

# Synthesis of Helical and Planar Extended-Phenanthridinium Salts

Valeriia Hutskalova,<sup>a</sup> Alessandro Prescimone,<sup>b</sup> and Christof Sparr<sup>\*a</sup>

<sup>a</sup> Department of Chemistry, University of Basel, St. Johannis-Ring 19, CH-4056 Basel, Switzerland,  
e-mail: christof.sparr@unibas.ch

<sup>b</sup> Department of Chemistry, University of Basel, BPR 1096, Mattenstrasse 24a, CH-4058 Basel, Switzerland

Dedicated to Professor *E. Peter Kündig* on the occasion of his 75th birthday

© 2021 The Authors. Helvetica Chimica Acta published by Wiley-VHCA AG. This is an open access article under the terms of the Creative Commons Attribution Non-Commercial License, which permits use, distribution and reproduction in any medium, provided the original work is properly cited and is not used for commercial purposes.

The investigation of new synthetic routes towards positively charged *N*-heterocycles is of high importance for the further development of medicinal chemistry, functional materials, catalysis and other areas of application. For accessing acridinium dyes, we previously reported an approach based on an aryne-imine-aryne coupling followed by the subsequent oxidation of the acridane intermediates. Herein, we now present an unusual reaction outcome when phenanthryne is used as aryne component. Under optimized conditions, this two-step synthetic methodology led to the formation of a helical tetrabenzophenanthridinium derivative. Furthermore, the susceptibility of this product to photoinduced cyclodehydrogenation was observed, providing a highly fluorescent planar polycyclic aromatic hydrocarbon with a positively charged nitrogen. The photophysical and electrochemical properties of the mesityl-phenyltetrabenzophenanthridinium tetrafluoroborate were also determined.

**Keywords:** arynes, cycloaddition, helicenes, nitrogen heterocycles.

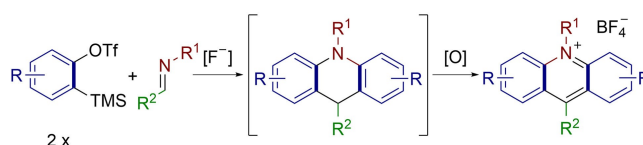
## Introduction

Tremendous advances in the field of nitrogen-based heterocyclic chemistry achieved over the last decades led to a broad range of applications for pharmaceuticals, agrochemicals, dyes, functional materials, and many more.<sup>[1–3]</sup> Acridinium salts are particularly useful scaffolds and have emerged as an efficient and sustainable class of cationic organic photocatalysts.<sup>[4–6]</sup> In recent studies, we investigated a short two-step route towards diverse acridinium salts involving the aryne-imine-aryne coupling reaction<sup>[7]</sup> followed by the subsequent oxidation of the acridane intermediate (Scheme 1,a).<sup>[8,9]</sup>

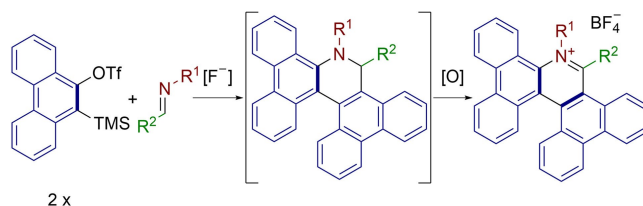
Herein, we now disclose the utilization of this methodology for larger polycyclic aryne substrates. The unique reactivity of arynes containing an extended  $\pi$ -system under typical aryne-imine-aryne

coupling conditions thereby lead to the notable formation of the tetrabenzophenanthridinium system (Scheme 1,b).

a) Our previous work: the Aryne-Imine-Aryne coupling for Acridiniums<sup>[7–9]</sup>



b) This work:



**Scheme 1.** Background and scope of the work.

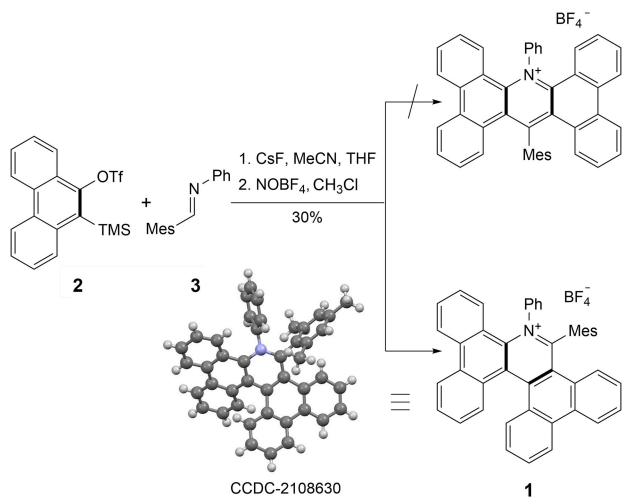
Supporting information for this article is available on the WWW under <https://doi.org/10.1002/hlca.202100182>

## Results and Discussion

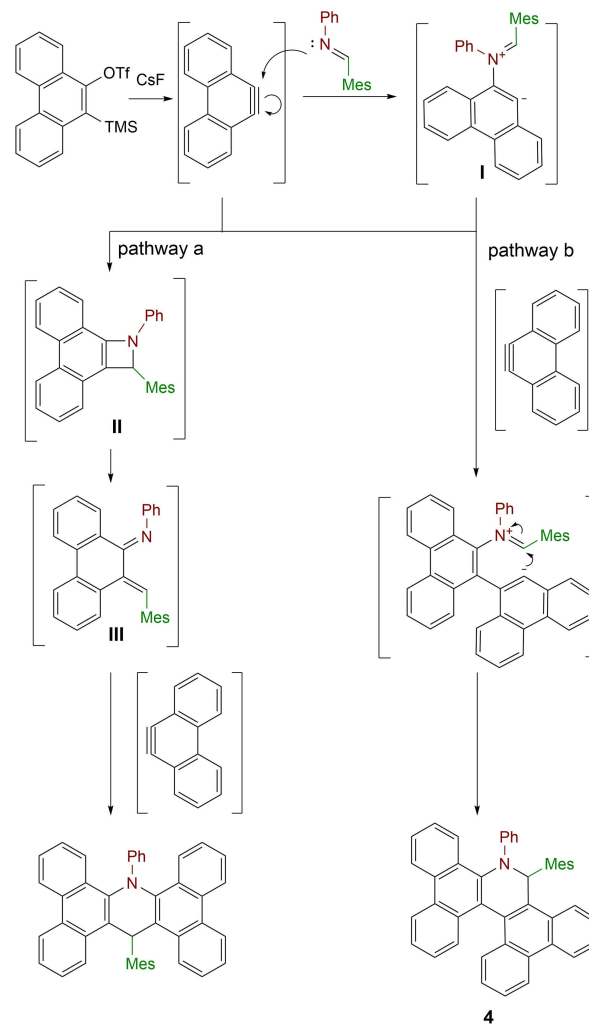
We started our investigation of the aryne-imine-aryne coupling reaction with polycyclic arynes by selecting the *Kobayashi* aryne precursor 10-trimethylsilylphenanthryl 9-trifluoromethanesulfonate **2** and imine **3** as suitable starting materials and then proceeded to their synthesis utilizing standard procedures.<sup>[10]</sup> Having the required compounds **2** and **3** in hand, we centered our attention on the aryne-imine-aryne coupling under conditions comparable to the two-step acridinium synthesis (Scheme 2).

Interestingly, upon NOBF<sub>4</sub>-mediated oxidation of the intermediate obtained from imine **3** and the aryne generated from precursor **2**, we observed that not the acridinium salt, but 18-mesityl-17-phenyltetrabenzo[*a,c,i,k*]phenanthridin-17-ium tetrafluoroborate **1** was formed.

Notably, the aryne-imine-aryne coupling reaction was described to proceed through the formation of aza-*ortho*-quinone methide intermediate **III**, which then reacts with the corresponding aryne to form a product possessing an acridane core (Scheme 3, pathway a).<sup>[7]</sup> However, in the case of phenanthryne, the formation of 1,2-dihydrobenzoazete **II** and intermediate **III** might be impacted by unfavorable steric interactions between the mesityl group and the extended system of the phenanthrene moiety. This increased steric bulk around the reactive center of phenanthryne could lead to a divergent mechanism of the aryne-imine-aryne coupling, which involves the nucleophilic attack of the imine at the phenanthryne, leading to the generation of intermediate **I**. A reaction



**Scheme 2.** Synthesis of 18-mesityl-17-phenyltetrabenzo[*a,c,i,k*]phenanthridin-17-ium tetrafluoroborate **1**.



**Scheme 3.** Possible pathways for the aryne-imine-aryne coupling to the acridane (pathway a) and the dihydrotetrabenzo-phenanthridine product **4** (pathway b).

with a second phenanthryne would subsequently result in the 17,18-dihydrotetrabenzo[*a,c,i,k*]phenanthridine derivative **4** (Scheme 3, pathway b).

To our delight, oxidation of the obtained compound **4** with nitrosonium tetrafluoroborate gave the final product **1** with a 30% yield over two steps. The structure of the corresponding product was confirmed by NMR spectroscopy and X-ray crystallography. Remarkably, compound **1** displays a helical structure within an *ortho*-condensed aromatic motif and can therefore be viewed as a 7-aza[5]helicium derivative.<sup>[11,12]</sup> It was earlier shown that monoaza[5]helicenes rapidly racemize at room temperature and that racemization barriers are lower than for the corresponding carbon analogues.<sup>[13]</sup> Furthermore, the position of the nitrogen significantly impacts the

configurational stability<sup>[14]</sup> and relatively low barriers were observed for the racemization of cationic diaza[5]helicenes.<sup>[15]</sup> We thus examined the racemization of the synthesized compound **1** after separation by HPLC on a chiral stationary phase. A sample of enantio-enriched **1** in acetonitrile was heated to 40 °C and the racemization was monitored by HPLC (Figure 1). Interestingly, besides confirming substantial racemization after 18 hours, the formation of another compound (**5**) was also observed.

Considering the tendency of [5]helicenes to undergo either light- or oxidant-promoted cyclodehydrogenation resulting in the formation of planar products,

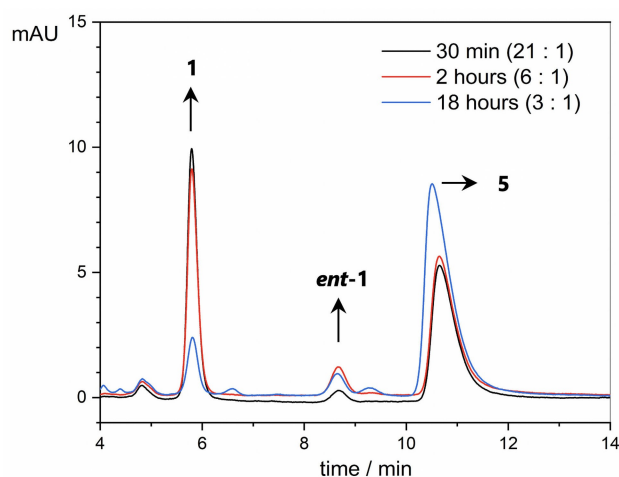


**Figure 1.** Overlay of HPLC traces for the thermal isomerization of **1** at 40 °C (*Chiralcel OJ-RH* was used as chiral stationary phase).

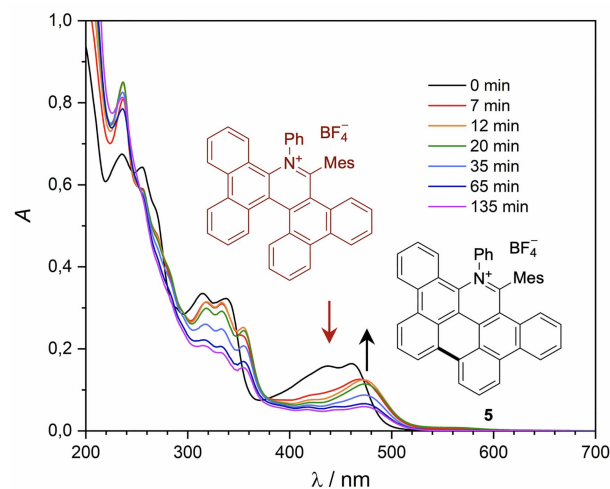
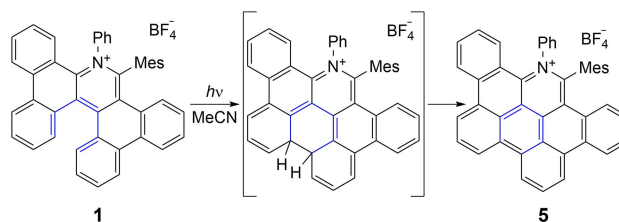


**Figure 2.** Changes in absorption spectra of **1** in dry degassed MeCN (15 μm) upon irradiation with blue LED light (*Kessil PR160L-467 nm*, 44 W, 25 % intensity).

we assumed that the appearance of the new signal in the HPLC data could be rationalized by a cyclization process.<sup>[16–22]</sup> We therefore turned to photostability studies of compound **1** using UV-visible absorption spectroscopy. Irradiation of a degassed solution of **1** in acetonitrile ( $\lambda_{\text{max}} = 467 \text{ nm}$ ) resulted in significant change of the absorption spectra, indicating the formation of a compound which was assigned to the nitrogen containing, positively charged, polycyclic aromatic hydrocarbon **5** (PAH, Figure 2). High-resolution mass spectrometry (HR-MS) of a solution obtained after two hours of irradiation further supported the photocyclodehydrogenation process yielding in compound **5**.

A plausible mechanism for this reaction involves the formation of the partially planarized cyclic intermediate which gives access to the final product **5** after hydrogen abstraction (Scheme 4).

Further support for this ring-closure was obtained from emission spectra of a freshly prepared degassed solution of **1** in acetonitrile and the same solution after 30 min irradiation (467 nm, Figure 3). Since only



**Scheme 4.** Photocyclodehydrogenation to the nitrogen containing PAH salt **5**.

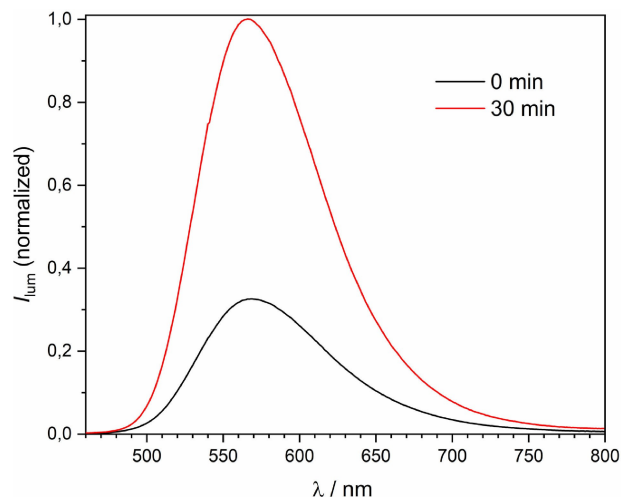


**Figure 3.** Alterations in the emission spectra of the degassed solution of **1** in acetonitrile (15 μm) upon irradiation with blue LED light (*Kessil PR160L-467 nm*, 44 W, 25 % intensity).

the emission intensity but not the  $\lambda_{\text{max}}$  changed over time, the emission throughout the measurements was assigned to the cyclic product **5** so that a non-emissive 7-aza[5]helicene derivative **1** is converted to the highly fluorescent compound **5** upon light illumination during the measurement.

We next examined the redox chemistry of the synthesized tetrabenzo[*a,c,i,k*]phenanthridin-17-ium derivative **1**. The cyclic voltammogram of **1** in dry degassed acetonitrile reveals a ground state reduction potential  $E_{1/2}$  of  $-0.48$  V against SCE with a scan rate of 1 V/s. Notably, a possible oxidative cyclodehydrogenation leading to compound **5** is also reflected by the voltammograms collected at different scan rates (Figure 4). A non-linear dependency of the peak currents on the square root of the scan rate along with the change of the voltammogram shape indicates, that the electron transfer is coupled with the reaction of the helically shaped tetrabenzo[*a,c,i,k*]phenanthridin-17-ium system (**1**).

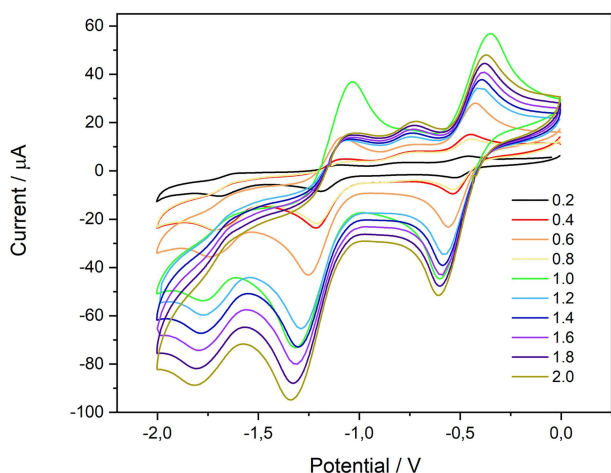
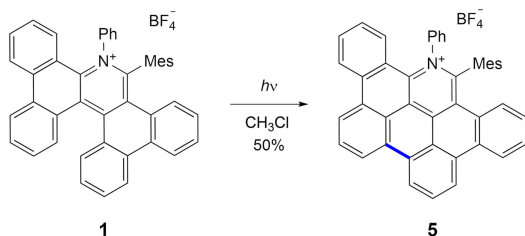


**Figure 4.** Cyclic voltammograms of **1** in deaerated  $0.1 \text{ mol L}^{-1}$  tetra-*n*-butylammonium hexafluorophosphate in MeCN measured at different scan rates between 0.2 and 2 V/s.



**Scheme 5.** Light-promoted cyclodehydrogenation of **1** ( $h\nu =$  Kessil PR160L-467 nm, 44 W, 25% intensity, 10 cm distance from the light source).

To support the notion of a cyclodehydrogenation, we performed the light-promoted cyclization on a scale sufficient to isolate product **5**. To our delight, the reaction was successfully carried out on  $15 \mu\text{mol}$  scale, yielding the desired product **5** with 50% yield after an operationally simple isolation by filtration of the clean product that precipitated during the reaction (Scheme 5). Overall, this methodology with an alternative reaction path of the aryne-imine-aryne coupling provides a practical route to both the helical tetrabenzo[*a,c,i,k*]phenanthridin-17-ium system (**1**) and the planar nitrogen containing PAH salt dibenzophenanthrophenanthridin-15-ium tetrafluoroborate (**5**).

## Conclusions

In conclusion, we describe that the larger polycyclic structure of phenanthryne in the aryne-imine-aryne coupling leads to a unique reaction pathway and the formation of a tetrabenzophenanthridinium salt upon oxidation. The photophysical and electrochemical properties of this helically shaped product were determined and a light-promoted cyclodehydrogenation was observed. The formation of the planar cyclic nitrogen containing polycyclic aromatic hydrocarbon highlights the capacity of the aryne-imine-aryne coupling for the rapid synthesis of larger nitrogen heterocycles and cationic polycyclic aromatic hydrocarbons.

## Experimental Section

### General Information

All reaction solvents and reagents were obtained from commercial suppliers and were used without further purification unless stated otherwise. Solvents for extractions and chromatography were technical grade. Syringes were used to transfer air and moisture sensitive liquids and solutions. Analytical thin layer chromatography (Merck silica gel 60 F254 plates) was utilized for monitoring reactions visualized by UV light (254 nm and 350 nm). Flash chromatography was performed with SiliCycle silica gel 60 (230–400 mesh). Concentration *in vacuo* was performed by rotary evaporation to *ca.* 10 mbar at  $40^\circ\text{C}$  and drying at *ca.*  $10^{-2}$  mbar at room temperature.  $^1\text{H-NMR}$  spectra were recorded on Bruker DPX 400 MHz or Bruker DRX 500 MHz spectrometers at 298 K in the indicated deuterated solvent supplied by Cambridge Isotope Laboratories. Chemical shifts ( $\delta$ ) are reported in parts

per million [ppm] and referenced to the residual solvent peak ( $\delta = 7.26$  ppm for  $\text{CDCl}_3$  and 1.94 ppm for  $\text{CD}_3\text{CN}$ ). The multiplicities are reported in Hz as: *s* = singlet, *br.* = broad singlet, *d* = doublet, *t* = triplet, *q* = quartet, *m* = multiplet.  $^{13}\text{C}$ - and 2D-NMR spectra were recorded with  $^1\text{H}$ -decoupling on Bruker DRX 500 MHz spectrometers at 298 K in the indicated deuterated solvent supplied by Cambridge Isotope Laboratories. Chemical shifts ( $\delta$ ) are reported in parts per million [ppm] and referenced to the residual solvent peak ( $\delta = 77.16$  ppm for  $\text{CDCl}_3$  and 1.32/118.26 ppm for  $\text{CD}_3\text{CN}$ ).

Melting points were measured on a Büchi B-565 melting point apparatus. IR spectroscopy was measured on an ATR Varian Scimitar 800 FT-IR spectrometer and reported in  $\text{cm}^{-1}$ . The intensities of the bands are reported as: *w* = weak, *m* = medium, *s* = strong. High-resolution mass spectrometry (HR-ESI) was recorded by Dr. Michael Pfeffer of the University of Basel on a Bruker MaXis 4G QTOF ESI mass spectrometer.

Photocatalytic transformations were performed using the following conditions: The vial was placed on a stirring plate, laterally in 10 cm distance to a Kessil PR160L-467 nm 44 W lamp, adjusted to 25% intensity. A sideward fan was used to keep temperature at ca. 30 °C.

HPLC data was collected using a Chiralcel OJ-RH column (5  $\mu\text{m}$ , 150  $\times$  4.6 mm) and  $\text{H}_2\text{O}/\text{MeCN}$  solvent system at 20 °C.

#### Steady-State Measurements

All steady-state absorption and luminescence spectra were measured using a Cary 5000 spectrometer from Varian and a Jasco FP-8600 with Jasco ETC-815 Peltier thermostated cell holder at 25 °C in a 1 cm cuvette. The solutions used for luminescence spectroscopy were sufficiently diluted to avoid filter effects.

#### Cyclic Voltammetry (CV)

Cyclic Voltammetry was performed in dry, degassed 0.1  $\text{mol L}^{-1}$  tetra-*n*-butylammonium hexafluorophosphate in MeCN (or other solvents if noted). Voltammograms were recorded with a Versastat3-200 potentiostat from Princeton Applied Research employing a glassy carbon disk working electrode, SCE reference electrode and a silver wire counter electrode. The glassy carbon electrode and Ag wire were polished prior to measurement.

#### Precursor Synthesis

**10-(Trimethylsilyl)phenanthren-9-yl Trifluoromethanesulfonate (2).** Step 1: Prepared according to the literature procedure starting from phenanthren-9-ol (2.00 g, 10.3 mmol) to yield the product as a white solid (1.45 g, 5.31 mmol, 52%). NMR corresponds to the literature data.<sup>[10]</sup>

Step 2: Prepared according to the literature procedure<sup>[23]</sup> starting from 10-bromophenanthren-9-ol (1.45 g, 5.31 mmol) to give the product as an orange solid (1.81 g, 4.54 mmol, 86%). NMR corresponds to the literature data.<sup>[10]</sup>

***N*-Phenyl-1-(2,4,6-trimethylphenyl)methanimine (3).** Aniline (1.40 g, 15.0 mmol), mesityl aldehyde (1.48 g, 10 mmol), and *p*-TsOH· $\text{H}_2\text{O}$  (95.0 mg, 500  $\mu\text{mol}$ ) were dissolved in 20 mL of dry toluene. 4 Å Molecular sieves were added to the obtained solution. The reaction mixture was refluxed for 18 h. The volatiles were removed under reduced pressure (5 mbar) and subsequently under high vacuum (< 0.1 mbar, 60 °C, to remove excess of aniline) to yield product **3** as a beige solid (2.07 g, 9.29 mmol, 93%). NMR corresponds to the literature data.<sup>[24]</sup>

**18-Mesityl-17-phenyltetrabenzo[*a,c,i,k*]phenanthridin-17-ium Tetrafluoroborate (1).** 10-(Trimethylsilyl)phenanthren-9-yl trifluoromethanesulfonate (117 mg, 290  $\mu\text{mol}$ ) was dissolved in dry THF (0.6 mL) and added in one portion to a mixture of anhydrous CsF (163 mg, 1.07 mmol), 1-mesityl-*N*-phenylmethanimine (**3**, 30.0 mg, 134  $\mu\text{mol}$ ), and dry acetonitrile (1.4 mL). After 16 h, the solvent was removed under reduced pressure, the residue dissolved in  $\text{CH}_2\text{Cl}_2$  (30 mL) and washed with water (30 mL). The aqueous phase was extracted with  $\text{CH}_2\text{Cl}_2$  (2  $\times$  10 mL), the combined organic layers were dried over  $\text{Na}_2\text{SO}_4$  and the solvent was removed under reduced pressure. The residue was purified by preparative thin layer chromatography over silica gel (cyclohexane/ $\text{Et}_2\text{O}$ , 20:1,  $R_f$  0.61). The obtained intermediate was dissolved in dry  $\text{CH}_2\text{Cl}_2$  (10 mL) and nitrosonium tetrafluoroborate (31.3 mg, 268  $\mu\text{mol}$ ) was added. The mixture was stirred for 1 h at ambient temperature, was diluted with  $\text{CH}_2\text{Cl}_2$  (10 mL) and washed with water (20 mL). The aqueous phase was extracted with  $\text{CH}_2\text{Cl}_2$  (2  $\times$  10 mL), the combined organic layers dried over  $\text{Na}_2\text{SO}_4$  and the solvent removed under reduced pressure to give the product **1** as a red solid after oxidation (25.7 mg, 39.0  $\mu\text{mol}$ ).

30%, decomp. at 193.2 °C). IR (neat): 3648w, 3067w, 2920w, 1728w, 1606w, 1571w, 1524m, 1446m, 1388m, 1342m, 1264w, 1217w, 1174w, 1047s, 860w, 753s, 727s, 860w, 753s, 727s, 695s, 657w, 613w. <sup>1</sup>H-NMR (500 MHz, CDCl<sub>3</sub>): 8.68 (2 H, *dd*, <sup>3</sup>*J* = 16.8, 8.2, C4H, C12H); 8.61 (2 H, *dd*, <sup>3</sup>*J* = 8.2, 3.2, C13H, C5H); 8.36 (1 H, *d*, <sup>3</sup>*J* = 8.3, C8H); 8.25 (1 H, *d*, <sup>3</sup>*J* = 8.3, C9H); 7.87 (1 H, *t*, <sup>3</sup>*J* = 7.5, C6H); 7.83–7.69 (3 H, *m*, C3H, C11H, C14H); 7.51–7.38 (4 H, *m*, C3''H, C5''H, C10H, C7H); 7.36–7.27 (5 H, *m*, C4''H, C6''H, C1H, C2H, C15H); 7.26–7.17 (1 H, *m*, C16H); 7.14 (1 H, *dd*, <sup>3</sup>*J* = 7.9, 1.9, C2''H); 6.95 (1 H, *s*, C3'H); 6.85 (1 H, *s*, C5'H); 2.32 (3 H, *s*, C4'-CH<sub>3</sub>); 1.96 (3 H, *s*, C6'-CH<sub>3</sub>); 1.81 (3 H, *s*, C2'-CH<sub>3</sub>). <sup>13</sup>C-NMR (126 MHz, CDCl<sub>3</sub>): 154.2 (C18); 142.7 (C8b); 142.0 (C4'); 141.2 (C1''); 138.6 (C18b); 136.4 (C2'); 136.3 (C6'); 134.2 (C6); 134.1 (C4b); 134.0 (C16a); 132.8 (C8); 132.0 (C4a); 131.1 (C3); 131.09 (C16b); 131.0 (C11); 130.56 (C14); 130.5 (C1'); 130.4 (C3'); 130.3 (C8d); 130.1 (C9); 129.9 (C4''); 129.7 (C3''); 129.5 (C5'); 129.1 (C15); 128.9 (C1); 128.5 (C18a); 128.4 (C16); 128.1 (C12a); 128.0 (C7); 127.8 (C5''); 127.5 (C10); 127.3 (C2''); 126.3 (C18c); 126.0 (C2); 125.6 (C8a); 125.4 (C6''); 124.5 (C12, C4); 124.4 (C5); 124.0 (C13); 121.9 (C12b); 21.3 (C4'-CH<sub>3</sub>); 20.8 (C6'-CH<sub>3</sub>); 20.4 (C2'-CH<sub>3</sub>). <sup>19</sup>F-NMR (376 MHz, CDCl<sub>3</sub>): -154.29; -154.34. HR-ESI-MS: 574.2533 (C<sub>44</sub>H<sub>32</sub>N<sup>+</sup>, M<sup>+</sup>; calc. 574.2529).

**16-Mesityl-15-phenyldibenzo[*c,i*]phenanthro[1,10,9,8-*klmna*]phenanthridin-15-ium Tetrafluoroborate (5).** 18-Mesityl-17-phenyltetrabenzo[*a,c,i,k*]phenanthridin-17-ium tetrafluoroborate (1; 9.92 mg, 15.0 μmol) was dissolved in deuterated chloroform (1.0 mL). Argon was bubbled through the solution for approximately 3 min, and the resulting mixture was stirred and irradiated for 23 h with a *Kessil PR160L-467 nm* lamp (44 W, 25% intensity, 10 cm distance from the light source). According to the NMR, no starting material was left. The precipitate formed during the reaction was collected, washed with cold chloroform and dried under reduced pressure to yield the product as an orange solid (4.92 mg, 7.46 μmol, 50%, decomp. at 309 °C). IR (neat): 3065w, 2922w, 1602w, 1600w, 1531w, 1459m, 1394m, 1340w, 1279w, 1230w, 1223w, 1057s, 859w, 763m, 710w. <sup>1</sup>H-NMR (500 MHz, CD<sub>3</sub>CN): 8.82 (1 H, *d*, <sup>3</sup>*J* = 7.7, C8H); 8.79 (1 H, *d*, <sup>3</sup>*J* = 7.9, C7H); 8.75 (1 H, *d*, <sup>3</sup>*J* = 8.2, C4H); 8.73–8.69 (2 H, *m*, C5H, C10H); 8.67 (1 H, *d*, <sup>3</sup>*J* = 7.8, C11H); 8.43 (1 H, *dd*, <sup>3</sup>*J* = 8.5, <sup>4</sup>*J* = 1.3, C14H); 8.07 (1 H, *t*, <sup>3</sup>*J* = 7.9, C6H); 7.98 (1 H, *t*, <sup>3</sup>*J* = 7.7, C9H); 7.90–7.85 (2 H, *m*, C3H, C10H); 7.84 (1 H, *dd*, <sup>3</sup>*J* = 8.5, <sup>4</sup>*J* = 1.2, C1H); 7.55 (1 H, *ddd*, <sup>3</sup>*J* = 8.5, <sup>3</sup>*J* = 7.0, <sup>4</sup>*J* = 1.2, C13H); 7.46 (*ddd*, <sup>3</sup>*J* = 8.4, <sup>4</sup>*J* = 6.9, <sup>4</sup>*J* = 1.3, C2H); 7.28–7.20 (1 H, C4''H); 7.14–7.05

(4 H, *m*, C2''H, C3''H, C5''H, C6''H); 7.03 (2 H, *s*, C3'H, C5'H); 2.36 (3 H, *s*, C4'-CH<sub>3</sub>); 1.94 (6 H, *s*, C2'-CH<sub>3</sub>, C6'-CH<sub>3</sub>). <sup>13</sup>C-NMR (126 MHz, CD<sub>3</sub>CN): 153.8 (C16); 145.5 (C1''); 143.1 (C4'); 142.1 (C14b); 138.5 (C2', C6'); 134.8 (C14b<sup>1</sup>); 134.5 (C16a); 133.8 (C6); 133.5 (C4b); 132.9 (C12); 132.8 (C7a); 132.6 (C4a); 132.3 (C1'); 131.3 (C3); 131.0 (C4''); 130.7 (C9); 130.6 (C14); 130.3 (C3', C5'); 129.9 (C7b); 129.8 (C10b); 129.6 (C2'', C6''); 129.45 (C3'', C5''); 129.4 (C2); 128.7 (C13); 128.1 (C1); 127.8 (C16b); 125.7 (C4); 125.6 (C11); 125.3 (C8); 125.2 (C10a); 125.1 (C10); 124.5 (C14a); 124.1 (C7); 124.0 (C5); 122.2 (C16a<sup>1</sup>); 120.8 (C4b<sup>1</sup>); 120.0 (C7b<sup>1</sup>); 21.4 (C4'-CH<sub>3</sub>); 21.3 (C2'-CH<sub>3</sub>, C6'-CH<sub>3</sub>). ESI-MS: 572.2376 (C<sub>44</sub>H<sub>30</sub>N<sup>+</sup>, M<sup>+</sup>; calc. 572.2373).

## Acknowledgements

We acknowledge the *Alfred Werner Fund* and the University of Basel for generous financial support. We are grateful to *Björn Pfund* and Prof. *Oliver S. Wenger* for their advice and the use of equipment to measure photophysical and electrochemical data. We thank Prof. Dr. *Michal Juríček* for fruitful discussions. Open access funding was provided by the University of Basel.

## Author Contribution Statement

*V. H.* and *C. S.* conceived the study, designed the experiments and analyzed the data. *V. H.* performed the experiments. *A. P.* carried out the X-ray crystallographic analysis. *V. H.* and *C. S.* wrote the manuscript.

## References

- [1] E. Vitaku, D. T. Smith, J. T. Njardarson, 'Analysis of the Structural Diversity, Substitution Patterns, and Frequency of Nitrogen Heterocycles among U.S. FDA Approved Pharmaceuticals', *J. Med. Chem.* **2014**, *57*, 10257–10274.
- [2] M. M. Heravi, V. Zadsirjan, 'Prescribed drugs containing nitrogen heterocycles: an overview', *RSC Adv.* **2020**, *10*, 44247–44311.
- [3] C. Lamberth, 'Heterocyclic chemistry in crop protection', *Pest Manage. Sci.* **2013**, *69*, 1106–1114.
- [4] A. Tlili, S. Lakhdar, 'Acridinium Salts and Cyanoarenes as Powerful Photocatalysts: Opportunities in Organic Synthesis', *Angew. Chem. Int. Ed.* **2021**, *60*, 19526–19549.
- [5] A. Vega-Peñalosa, J. Mateos, X. Companyó, M. Escudero-Casao, L. Dell'Amico, 'A Rational Approach to Organophotocatalysis: Novel Designs and Structure-Property Relationships', *Angew. Chem. Int. Ed.* **2021**, *60*, 1082–1097.

- [6] N. A. Romero, D. A. Nicewicz, 'Organic Photoredox Catalysis', *Chem. Rev.* **2016**, *116*, 10075–10166.
- [7] H. Yoshida, H. Kuriki, S. Fujii, Y. Ito, I. Osaka, K. Takaki, 'Aryne-Imine-Aryne Coupling Reaction via [4+2] Cycloaddition between Aza-*o*-Quinone Methides and Arynes', *Asian J. Org. Chem.* **2017**, *6*, 973–976.
- [8] V. Hutskalova, C. Sparr, 'The Versatility of the Aryne-Imine-Aryne Coupling for the Synthesis of Acridinium Photocatalysts', *Synlett* **2021**, doi: 10.1055/s-0040–1720349.
- [9] V. Hutskalova, C. Sparr, 'Ad Hoc Adjustment of Photoredox Properties by the Late-Stage Diversification of Acridinium Photocatalysts', *Org. Lett.* **2021**, *23*, 5143–5147.
- [10] D. Peña, D. Perez, E. Guitián, L. Castedo, 'Selective Palladium-Catalyzed Cocyclootrimerization of Arynes with Dimethyl Acetylenedicarboxylate: A Versatile Method for the Synthesis of Polycyclic Aromatic Hydrocarbons', *J. Org. Chem.* **2000**, *65*, 6944–6950.
- [11] Y. Shen, C.-F. Chen, 'Helicenes: Synthesis and Applications', *Chem. Rev.* **2012**, *112*, 1463–1535.
- [12] K. Xu, Y. Fu, Y. Zhou, F. Hengersdorf, P. Machata, I. Vincon, J. J. Weigand, A. A. Popov, R. Berger, X. Feng, 'Cationic Nitrogen-Doped Helical Nanographenes', *Angew. Chem. Int. Ed.* **2017**, *56*, 15876–15881.
- [13] R. H. Janke, G. Haufe, E.-U. Würthwein, J. H. Borkent, 'Racemization Barriers of Helicenes: A Computational Study', *J. Am. Chem. Soc.* **1996**, *118*, 6031–6035.
- [14] T. Caronna, A. Mele, A. Famulari, D. Mendola, F. Fontana, M. Juza, M. Kamuf, K. Zawatzky, O. Trapp, 'Combined Experimental and Theoretical Study on the Stereodynamics of Monoaza[5]helicenes: Solvent-Induced Increase of the Enantiomerization Barrier in 1-Aza-[5]helicene', *Chem. Eur. J.* **2015**, *21*, 13919–13924.
- [15] M. Marinova, S. Pascal, L. Guénée, C. Besnard, B. Shivachev, K. Kostova, C. Villani, R. Franzini, V. Dimitrov, J. Lacour, 'Synthesis, Resolution, Configurational Stability, and Properties of Cationic Functionalized [5]Helicenes', *J. Org. Chem.* **2020**, *85*, 11908–11923.
- [16] P. Ravat, R. Hinkelmann, D. Steinebrunner, A. Prescimone, I. Bodoky, M. Juriček, 'Configurational Stability of [5] Helicenes', *Org. Lett.* **2017**, *19*, 3707–3710.
- [17] L. Liu, T. J. Katz, 'Bromine auxiliaries in photosyntheses of [5]helicenes', *Tetrahedron Lett.* **1991**, *32*, 6831–6834.
- [18] C. Shen, G. Zhang, Y. Ding, N. Yang, F. Gan, J. Crassous, H. Qiu, 'Oxidative cyclo-rearrangement of helicenes into chiral nanographenes', *Nat. Commun.* **2021**, *12*, 2786.
- [19] M. Juriček, 'The Three C's of Cethrene', *Chimia* **2018**, *72*, 322–327.
- [20] P. Ravat, T. Šolomek, D. Häussinger, O. Blacque, M. Juriček, 'Dimethylcethrene: A Chiroptical Diradicaloid Photoswitch', *J. Am. Chem. Soc.* **2018**, *140*, 10839–10847.
- [21] D. Wu, X. Feng, M. Takase, M. C. Haberecht, K. Müllen, 'Synthesis and self-assembly of dibenzo[*jk,mn*]naphtho[2,1,8-*fg*h]thebenidinium derivatives', *Tetrahedron* **2008**, *64*, 11379–11386.
- [22] M. Rosenberg, M. Santella, S. A. Bogh, A. V. Muñoz, H. O. B. Andersen, O. Hammerich, I. Bora, K. Lincke, B. W. Laursen, 'Extended Triangulenium Ions: Syntheses and Characterization of Benzo-Bridged Dioxo- and Diazatriangulenium Dyes', *J. Org. Chem.* **2019**, *84*, 2556–2567.
- [23] H. Jiang, Y. Zhang, W. Xiong, J. Cen, L. Wang, R. Cheng, C. Qi, W. Wu, 'A Three-Phase Four-Component Coupling Reaction: Selective Synthesis of *o*-Chloro Benzoates by KCl, Arynes, CO<sub>2</sub>, and Chloroalkanes', *Org. Lett.* **2019**, *21*, 345–349.
- [24] G. P. Junor, E. A. Romero, X. Chen, R. Jazzar, G. Bertrand, 'Readily Available Primary Aminoboranes as Powerful Reagents for Aldimine Synthesis', *Angew. Chem. Int. Ed.* **2019**, *58*, 2875–2878.

Received September 16, 2021

Accepted October 22, 2021